LAWRENCE
LIVERMORE
NATIONAL
LABORATORY

UCRL-JRNL-221689

Enchanced hohlraum radiation drive through reduction of wall losses with high-Z mixture "cocktail" wall materials

J. Schein, O. Jones, M. Rosen, E. Dewald, S. Glenzer, J. Gunther, B. Hammel, O. Landen, L. Suter, R. Wallace

May 30, 2006

Physics Review Letters

Enhanced hohlraum radiation drive through reduction of wall losses with high-Z mixture "cocktail" wall materials

Jochen Schein, Ogden Jones, Mordecai Rosen, Eduard Dewald, Siegfried Glenzer, Janelle Gunther, Bruce Hammel, Otto Landen, Laurence Suter , Russell Wallace

Lawrence Livermore National Laboratory, 7000 East Avenue, L-399, Livermore, CA

Abstract: We present results from experiments, numerical simulations and analytic modeling, demonstrating enhanced hohlraum performance. Care in the fabrication and handling of hohlraums with walls consisting of high-Z mixtures (cocktails) has led to our demonstration, for the first time, of a significant increase in radiation temperature (up to +7eV at 300 eV) compared to a pure Au hohlraum, in agreement with predictions and ascribable to reduced wall losses. The data extrapolated to full NIF suggest we can expect an 18% reduction in wall loss for the current ignition design by switching to cocktail hohlraums, consistent with requirements for ignition with 1MJ laser energy.

Increasing hohlraum coupling efficiency for ignition experiments at the National Ignition Facility (NIF) is desired to achieve ignition using laser driven inertial confinement fusion. Current designs show a threshold for ignition at a fixed energy of E_C=0.14MJ to be deposited into the fusion capsule in the center of hohlraum. To achieve this, a laser energy $E_{Laser} >> E_C$ has to be first deposited inside the hohlraum through Laser Entrance Holes (LEH), for which a large fraction (taking into account possible scattering losses $E_{Scatter}$,) is designed to be absorbed by the hohlraum wall and converted into x-rays with an efficiency η_{CE}. In indirect drive ignition using hohlraums only a fraction of the x-radiation directly produced will illuminate the capsule, since the majority will get absorbed and only partially reemitted by the hohlraum walls or escape through the LEH. Thus reducing the x-ray flux that is lost to the wall E_{wall} and through the LEH E_{LEH} increases the energy on the capsule, thereby allowing ignition at lower laser energy or providing increased margin for ignition at high laser energy, as described by the following energy balance equation.[1]

$$E_C = (E_{laser} - E_{Scatter})\eta_{CE} - E_{wall} - E_{LEH} \quad (1)$$

Once the x-radiation produced by the incident laser illuminates the wall, wall material is heated up by absorption, ablated and highly ionized resulting in re-emission and excited states. The fraction that is not re-emitted back into the hohlraum drives a thermal diffusion wave into the cold wall, the so-called Marshak wave [2]. The amount of energy that diffuses into the wall – the wall loss – depends on the heat capacity ε of the wall material and the amount of material heated. The areal mass of the heated material m_F is equal to the product of the penetration depth of the heat front x_M, (the Marshak depth) and the density of the material ρ. Assuming power law dependencies for the opacity

κ and specific heat as functions of temperature T, and for T as a function of time, an analytic similarity solution can be found for a subsonic heat front where the amount of heated mass is given by $m_F^2 \propto \sigma T^4 t / \kappa\varepsilon$. Typically results for κ and ε for Au can be found using a fit to more detailed equations of state [3,4]

$$\kappa_{Au}(cm^2 g^{-1}) = \kappa_0 \rho^{0.18} / T^{1.43} \qquad (\kappa_0=6544) \qquad (2)$$

$$\varepsilon_{Au}(MJ / g) = \varepsilon_0 T^{1.54} / \rho^{0.15} \qquad (\varepsilon_0=3.3) \qquad (3)$$

where T is in heV and ρ in g/cm^3. These equations describe a subsonic wall loss that includes an isothermal rarefaction treatment of ρ as [4]:

$$E_{wall} / A_{wall} = \int F dt = \sigma \int (1-\alpha) T^4 dt \sim \varepsilon \cdot \rho \cdot x_M \sim (\varepsilon_0^{\,0.7} / \kappa_0^{\,0.4}) T^{3.3}(t) \cdot t^{0.59} \quad (4)$$

Thus in order to reduce the wall loss, we need low specific heat and high opacity, which increases the albedo α and therefore leads to higher reemission and consequently, at fixed incident laser energy, higher T. Here F represents the heat flux absorbed by the wall. In addition we see from Eq. (1) that the wall material must also be chosen to provide sufficient conversion efficiency to ensure efficient production of x-rays.

Previous experiments have indicated [5-7] that wall opacity can be increased by using a combination of high-Z materials, "cocktails". These are typically fabricated by co-sputtering materials onto a substrate or by sequentially depositing individual thin layers whose thicknesses are much less than one radiation mean free path. The materials are chosen to provide overlapping energy bands to fill spectral ranges with low opacity of one material with high opacity in the same spectral range of another material, while still maintaining high average Z and thus low specific heat. By comparing the calculated wall losses for various combinations of materials irradiated by a time dependent radiation source from an ICF ignition hohlraum design, we found that a combination of 60% U

(alloyed with 6% of Nb), 20% Dy and 20% Au should provide significant reduction in wall loss. For this cocktail mixture the approximate power laws for κ and ε [4]are:

$$\kappa_{CT}(cm^2 g^{-1}) = 5670\rho^{0.1}/T^{0.9} = 0.86\rho^{-0.08}T^{0.53}\cdot\kappa_{Au} \qquad (5)$$

$$\varepsilon_{CT}(MJ/g) = 0.95\varepsilon_{Au} \qquad (6)$$

Figure 1 shows the cold opacities for Au and U and Dy from the CXRO data tables [9] The insert compares the warm Rosseland mean opacities of Au and CT as approximated by power law fits (Eqs. (2), (5)) in the temperature range of interest.

Using these equations we can now develop the analytical expressions for the wall loss [4,8], (*with E in hJ, A in mm^2, T in heV, t in ns*).

$$E_{wall\_Au} = A_{wall}\cdot 0.58\cdot T_0^{3.3}\cdot t^{0.59} \qquad (7)$$

for Au, assuming a constant radiation temperature $T(t)=T_0$ and

$$E_{wall\_CT} = A_{wall}\cdot 0.60\cdot T_0^{3.1}\cdot t^{0.57} \qquad (8)$$

for the cocktail described above. Equations (5), (7), (8) indicate that cocktails become more advantageous at higher radiation temperature scaling as $E_{CT}/E_{Au} \approx T(t)^{-0.2}$ predicting a wall loss ratio E_{wall_CT}/E_{wall_Au} of pure cocktail compared to pure Au of 92% for a radiation temperature of 180 eV, 84.5% for of 270 eV and 83% for 305 eV after t=1ns of a flat drive profile. In order to reach these values care has to be taken to avoid contamination of the cocktail with low Z material, which increases the heat capacity and thus the wall loss. For example, the addition of 40% oxygen to CT, which represents the bonding of one O atom to each U and Dy atom, increases the heat capacity of the CT material sufficiently to increase wall loss for cocktails by a factor of 1.07, significantly reducing the advantage of the cocktail.

We demonstrate the enhancement with cocktails by performing experiments at the Omega Laser Facility [10] in which we compared T of Au and cocktail hohlraums, driven with the same laser energy, since we believe past attempts at demonstrating an increase in T [11] may have been influenced by oxygen contamination. The amount of oxygen in the coating material was controlled by a new hohlraum manufacturing process. Also, improved material quality controls and new handling techniques were implemented. The new process employs a Au substrate hohlraum split in two along the hohlraum axis producing two shaped halves. A total of 5μm of cocktail material is co-sputtered onto the inside surface of the halves before re-assembly, which produces a well-mixed composition of U(Nb), Dy and Au and allows for easy characterization. The cocktail is then over-coated with 0.2 μm Au liner. This Au liner serves to prevent oxygen from getting to the cocktail material. All hohlraums used had a wall thickness of 100 μm for additional mechanical stability and the sizes were chosen to keep a constant LEH area/wall area ratio of 11%. The finished hohlraums were stored in nitrogen filled containers until one hour before each experiment. Figure 2 shows a schematic of the new method. The finished coatings were analyzed using Auger spectroscopy and it was found that the amount of oxygen directly underneath the 0.2 μm Au layer was 5-10%, which remained stable for weeks in a controlled nitrogen atmosphere, and is predicted to have just a small (2%) influence on the wall loss.

In order to test the physics model that predicts a scaling of cocktail performance as a function of radiation temperature T experiments were performed using scale 3/4 (2.06 mm long x 1.2 mm dia, 0.8 mm LEH) hohlraums driven by 20kJ of 3 ω laser energy for an expected T of 270eV and scale 3/4 hohlraums driven by a laser energy of 10kJ for an

expected T of 185 eV. The maximum T was achieved with scale 5/8 hohlraums driven by 20kJ for an expected T of 305 eV. The pulse length for all experiments was 1 ns. In order to calculate the expected improvements using the described hohlraums with cocktail walls we start from the energy balance eq. (1) modified to account for the fact that these hohlraums did not contain a capsule.

$$(E_{laser} - E_{Scatter})\eta_{CE} = E_{wall} + E_{LEH} \qquad (9)$$

with the LEH loss given by:

$$E_{LEH} = A_{LEH} \cdot \sigma \cdot \int T(t)^4 dt \qquad (10)$$

Calculations [4] show that η_{CE} increases as $t^{0.2}$. Thus Eq (9), with wall loss dominating, leads to a prediction, confirmed by empirical data, that a 1ns square pulse at Omega produces a radiation temperature which rises with $T \sim t^{0.18}$, which modifies eq. (7), (8) and (10) into [4]

$$E_{wall\_Au} = A_{wall} \cdot 0.39 \cdot T_0^{3.3} \cdot t^{1.18} \qquad (11)$$

$$E_{wall\_CT} = A_{wall} \cdot 0.42 \cdot T_0^{3.1} \cdot t^{1.13} \qquad (12)$$

$$E_{LEH} = A_{LEH} \cdot 0.58 \cdot T_0^{4} \cdot t^{1.72} \qquad (13)$$

with T_o describing the peak radiation temperature at the end of the pulse. Using Eq. (11) and (12) we obtain modified wall loss ratios of 93% (180eV), 86.5% (270eV) and 84.5% (305eV). These calculated data can be compared to radiation-hydrodynamics calculations using the code LASNEX, resulting in slightly higher losses of 96.7%, 88.6% and 86.1%. The simulations employ the actual laser pulse shape and measured LEH size and assume low backscatter as measured.

In addition to these wall losses we have to account for the influence of the 0.2 μm Au liner, which reduces the influence of the cocktail improvement on wall loss. The Marshak depth for a cocktail (*t=1, T_o=2.7*) is given by [4,12]:

$$m_F = 0.00088 \cdot T_0^{1.7} \cdot t^{0.8} / 19.3 = 2.5\mu\text{m}, \qquad (14)$$

thus predicting that for a 1ns pulse of 270eV about 21% of the energy is deposited into the 0.2μm layer of Au. Even though the Au liner thickness is only ~8% of the Marshak depth it contains much kinetic energy and significantly influences the radiation flow deeper into the wall. Thus the Au liner reduces the effectiveness of the cocktail hohlraum and changes the wall loss ratios for the present experiments to 96% (180 eV), 89.5% (270eV) and 87% (305 eV). Taking into account the additional small amount of oxygen measured in the wall will reduce the wall loss ratios further to 97% (180 eV), 90.5% (270eV) and 88% (305 eV). These values are very close to LASNEX results, taking into account the Au liner: 98% (180eV), 91.2% (270eV) and 88.6% (305eV).

The absolute flux was measured time resolved for all experiments using a broadband 10 channel soft x-ray spectrometer "Dante" [13] over an energy range from 0-5 keV. The radiation temperature was derived by integrating over the x-ray flux taking into account the effective x-ray source size given by the line of sight of Dante to the LEH. The error from absolute calibrations of Dante amounts to 3% in absolute T and 0.7 % in relative T, the latter ascribed to shot-to-shot laser energy uncertainty (1% in flux) and source size tolerances (2% in flux). The source size was monitored using a soft x-ray imager with 50ps temporal resolution.

Figure 3 shows the measured and LASNEX simulated time history of the radiation temperature together with the Dante spectrum for cocktail and Au hohlraum experiments

(scale 3/4, 20kJ). After initially applying the laser pulse, the inferred radiation temperature increases in ~300ps to a value of 230eV. Afterwards it continues to increase more slowly with time ($\sim t^{0.18}$) as assumed in the analytic model Eq (11)-(13). Both the experimental data and LASNEX show that the advantage of cocktail over pure Au is temperature and time dependent in agreement with predictions. The Dante spectrum at the peak of the drive (fig 3. insert) indicates that the cocktail is more advantageous below 2keV, whereas the strong M-band emission of Au cancels any advantage in the region above 2keV as expected [14]. This is consistent with integrated Dante flux measurements. We can define the M-band fraction as the ratio of the radiation flux between 2-5keV to the total flux, which is higher for pure Au in all experiments ranging from 20% at 305 eV for scale 5/8 to 6% for the 200eV hohlraums. The corresponding cocktail results are 17.5% and 5.5%, respectively. The flux above 2keV was analyzed by time integrated spectroscopy and it was found that while in the case of Au the radiation is mainly produced by Au M-band emission on top of the black body continuum the Cocktails show mostly U and Dy specific transitions above 3.5keV, with weaker Au lines as expected.

Additional diagnostics used were Full Aperture Backscattering (FABS) and Near Backscatter Imager (NBI) to determine the influence of backscattered laser energy from Laser Plasma Interactions (LPI) on T cocktail and Au hohlraums. With some defocusing of the laser beams the intensity at the LEH was adjusted to $2*10^{15}$ W/cm^2. The resulting backscattered to total laser energy fraction ranged from ca 7% for the smaller 300eV hohlraums to ca 1.5% in the 180eV case, with no difference between Au and cocktail. The backscattered laser energy due to Brillouin (SBS) and Raman (SRS) Scattering were

measured separately, with SBS being higher than SRS by at least a factor of 2. These findings indicate the lack of large quantities of low-Z impurities in these experiments.

Figure 4 shows the results of the flux measurements at the peak of the drive together with curves of expected increase in radiation temperature, based on Eqs (9),(12), allowing for various level of oxygen in the wall as a function of radiation temperature. The experimental results of this campaign show an increase in T of 1eV to 7eV in agreement with the analytical predictions for Au lined CT hohlraums with 10% oxygen concentration as measured by Auger spectroscopy. Each datapoint is the result of two experiments comparing a cocktail hohlraum to a corresponding Au hohlraum, with one datapoint (circled) lying significantly outside the prediction (figure 4). This may be due to insufficient thickness of the CT layer, which was not tested for this particular target.

We now extrapolate these results to the NIF ignition hohlraum drive which ends with a 3ns pulse yielding a 300 eV radiation temperature. The wall loss for a Au layered cocktail drops further than shown for the Omega experiments due to the time dependence of the wall loss ratio $E_{wrall\_CT}/E_{wall\_Au} \sim T_0^{-0.19} t^{-0.05}$ and the larger penetration depth of the Marshak wave (~8μm), which in turn greatly reduces the influence of the 0.2 μm Au liner. Thus for a NIF ignition pulse [15] we can expect to see the wall loss ratio reduced to 81% (no oxygen) and 82.5% (w/10% oxygen) for a slow rising $T \sim t^{0.18}$ pulse, providing the necessary energy margin to achieve ignition at 1MJ laser energy.

In summary we presented experiments demonstrating that by controlled target production and handling cocktail hohlraums can be manufactured with low oxygen content that lower the opacity without increasing the heat capacity to reduce the wall loss thus

producing results in very good agreement with modeling predictions and with important implications for ignition target performance on the NIF.

The authors wish to acknowledge the help and outstanding performance of the Omega team at the University of Rochester, G. Rochau from Sandia Nat. Lab. for his help during experiments, the Physics Dept. of LLNL for providing opacity and EOS data, and the computational support of the LLNL LASNEX team.

This work was performed under the auspices of the U.S. Department of Energy by UC, Lawrence Livermore National Laboratory under contract W-7405-Eng-48.

[1] J. D. Lindl, Phys. Plasmas **2**, 3933 (1995); J. D. Lindl *et al*., Phys. Plasmas **11**, 339 (2004).

[2] R.E. Marshak, Phys. Fluids, **1**, 24 (1958)

[3] M. D. Rosen, Lsr. Prg. Ann. Rep. LLNL, UCRL-50055-79 (1979)

[4] M.D. Rosen, Proc. Scottish Univ. Sum. School Phys. TBP UCRL PROC 215898 (2005)

[5] H. Nishimura et al., Appl. Phys. Lett. **62**, 12 (1993)

[6] D. Colombant et al., Phys. Rev. E. **57**, 3411 (1998)

[7] T. J. Orzechowski et al., Phys. Rev. Lett. **77**, 3345 (1996)

[8] J. H. Hammer, M.D. Rosen, Phys. Plasmas **10**, 1829 (2003)

[9] Lawrence Berkeley Nat. Lab. Center For X-Ray Optics. www.cxro.lbl.gov

[10] J. M. Soures, et al. Phys. Plasmas **3** (5), 2108 (1996).

[11] S. Glenzer, E. Dewald, O. Jones, private communications

[12] M.D. Rosen UCRL-Pres-214063-19

[13] H. N. Kornblum et al., Rev. Sci Inst. **57** (1986)

[14] O. Jones, private communications

[15] D. A. Callahan, et al., accepted for public. Phy. Plasmas (2006)

Figure Captions:

Figure 1: Frequency dependent cold opacity of cocktail materials using overlapping energy bands to fill low-opacity regions. Also shown (small insert) is the opacity of Au and cocktail (CT) between a radiation temperature of 150eV and 300eV according to an approximation described in Eqs. (2) (5) assuming a density of 1g/cc relevant to the experiments described in this paper.

Figure 2: Picture of new cocktail hohlraum before assembly. Also shown is the experimental setup including major diagnostics (blue arrows depict optical radiation, red arrows depict x-radiation)

Figure 3: T as function of time as modeled by LASNEX and compared to measurements (CT – squares, Au - circles). Also shown (small insert) are the spectra at 1.1 ns as measured by Dante for Au (solid) and CT (dashed).

Figure 4: Increase of radiation temperature as a function of radiation temperature. Measurements are shown with error bars, lines represent expected increase for cocktail wall, (no O_2 with Au liner– dotted line, 10% O_2 with Au liner – solid line, 40% O_2 with

Au liner – dashed line), LASNEX results for non-lined (triangles) and lined (crosses) cocktails are shown as well .

Figure 1 :

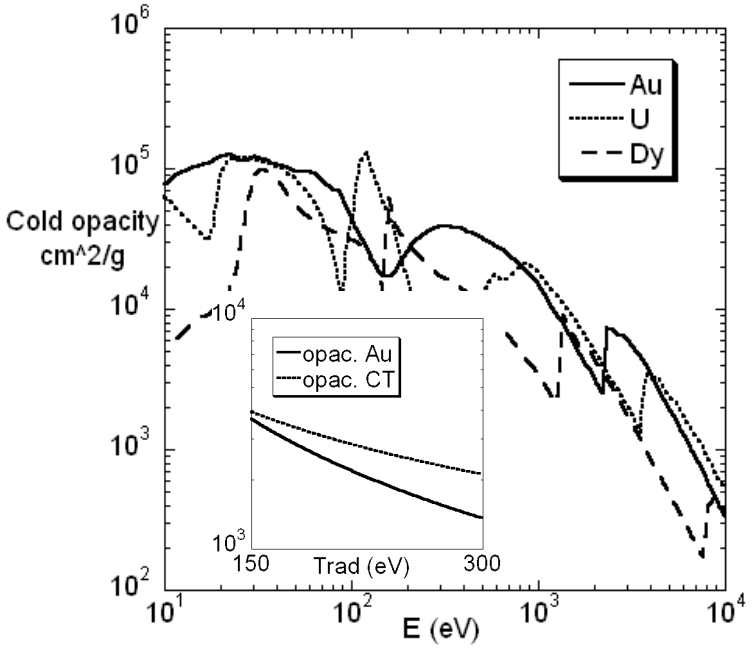

Figure 2 :

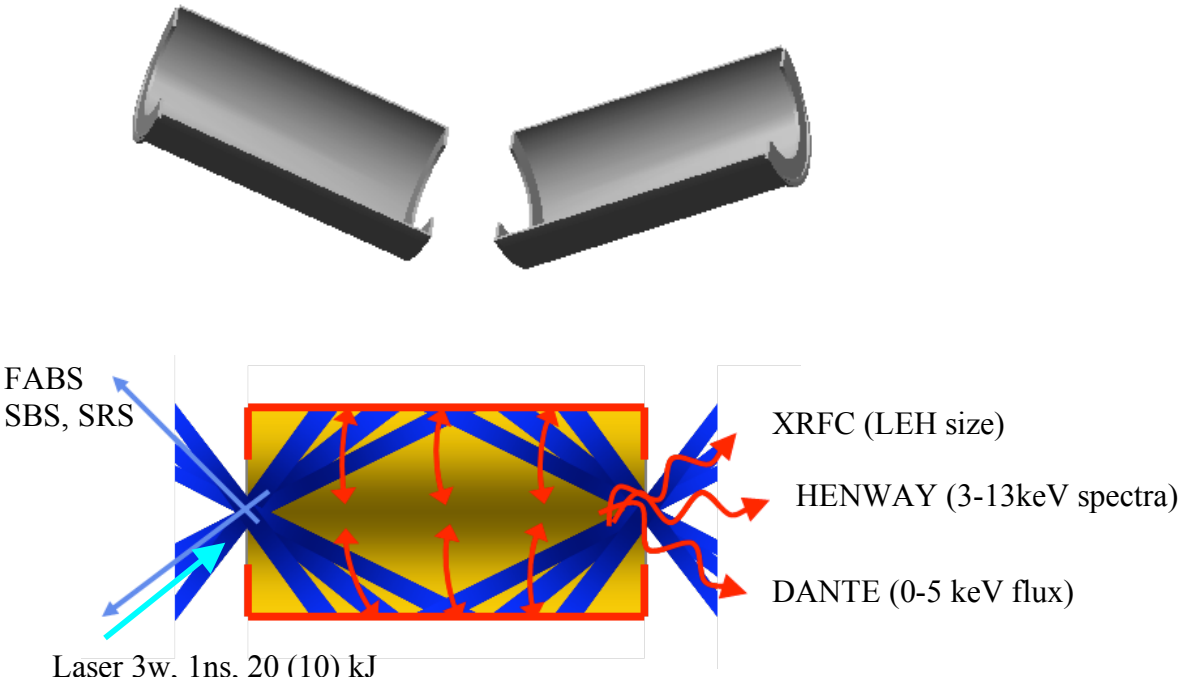
FABS
SBS, SRS
XRFC (LEH size)
HENWAY (3-13keV spectra)
DANTE (0-5 keV flux)
Laser 3w, 1ns, 20 (10) kJ

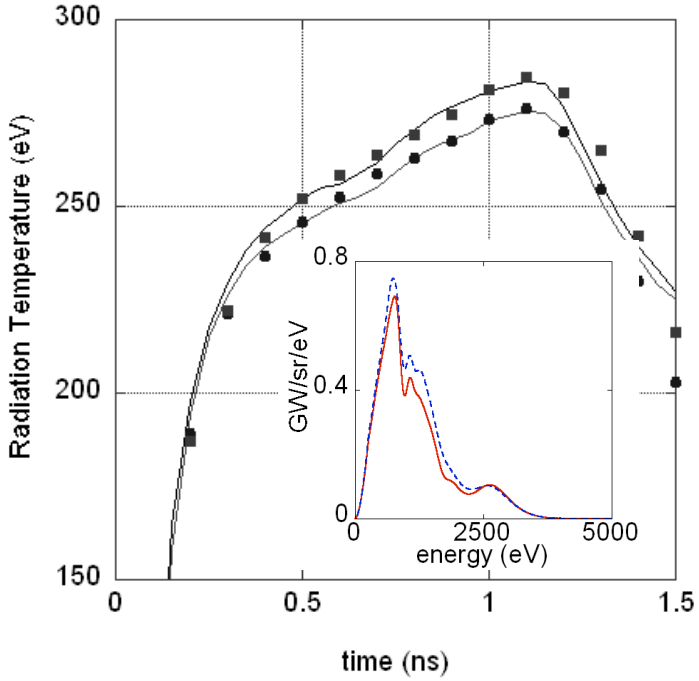
Radiation Temperature (eV)
300
250
200
150
0
0.5
1
1.5
time (ns)
0.8
0.4
0
GW/sr/eV
0
2500
5000
energy (eV)

Figure 3 :

Figure4

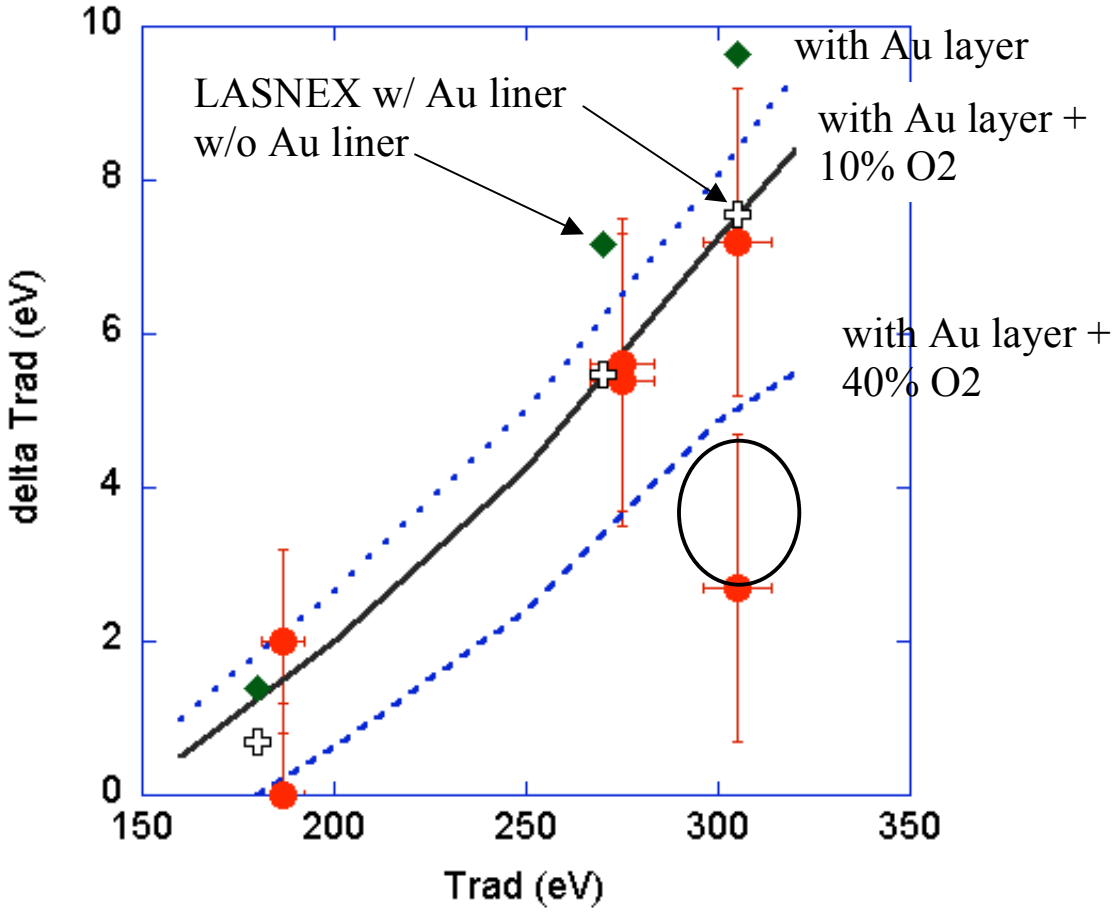
10
8
6
4
2
0
150
200
250
300
350
delta Trad (eV)
Trad (eV)
with Au layer
LASNEX w/ Au liner
w/o Au liner
with Au layer +
10% O2
with Au layer +
40% O2